Hybrid Cellular Automata for Manipulating Complex and Chaotic Cellular Automata

Brian LuValle

Control of chaos methods have been successfully applied to many small, closed, chaotic systems; however, there is a difficulty in expanding them to be applicable to large, open, chaotic systems. In this paper, a novel method of manipulating chaotic systems using hybrid cellular automata is proposed and evaluated. Four experiments are performed. The first experiment examines hybrid cellular automata in the presence of perturbations to the initial conditions. The second experiment analyzes the relationship between the total number of perturbations and the certainty that hybrid states will change. The third experiment analyzes the reachability of hybrid systems using complexity measures. The fourth experiment analyzes how phase transitions are affected by highimpact hybrid schemes.

Keywords: control of chaos; cellular automata; hybrid cellular automata; reachability; block entropy; structural entropy; block decomposition method; algorithmic information dynamics

1. Introduction

Chaotic and complex systems often have large nonlinear responses to miniscule changes in conditions. Control of chaos methods attempt to steer a system toward a desired behavior by giving calculated minute adjustments to the trajectory of a system in its dynamic attractor.

Hybrid cellular automata are proposed as a method of chaos control for real-world, open systems, specifically in cases where the manipulator wants to change a local state but not remove chaotic behavior from the general system.

1.1 Control of Chaos

Many proposed control of chaos applications involve a delicate balancing act of only perturbing the conditions when absolutely necessary. This is done under the physical interpretation of conserving energy. Unfortunately, in large enough systems, it becomes difficult to computationally determine these exact points in time.

In the presence of other introduced uncertainties, these small, intentional perturbations can be canceled out by noise. This is unfortunate

news for the practical implementation of chaos control in large-scale, open, real-world systems.

Recently, control of chaos has been applied to the Lorenz 63 model: a simplified model of atmospheric convection [1]. In that study, an oscillation around a single loop of the attractor was implemented using perturbations that were less than 3% of the size of the measurement error.

Control of chaos has also been applied in some cases to coupled lattice maps, which can be argued are a generalization of cellular automata. Many real systems that can be modeled as coupled lattice maps are impossible to control completely, and it would be much more beneficial to manipulate them locally into desired states.

Traditional control of chaos methods require large computations to determine the optimal control placement. Also, the control is reanalyzed at time steps much smaller than the Lyapunov time.

1.2 Hybrid/Nonuniform Cellular Automata

Hybrid/nonuniform cellular automata are cellular automata where the rules applied across the input are nonuniform. This has interesting implications for reachability and complexity of these hybrid systems [2].

An example of hybrid rule configuration is illustrated in Figure 1. The original cells are shown in white, and the hybrid cell is shown in red. Nonuniform cellular automata can demonstrate behavior that is not found in uniform cellular automata.

Figure 1. A rule scheme of a hybrid cellular automaton.

1.2.1 One-Dimensional Hybrid Cellular Automata

In one-dimensional hybrid cellular automata, the Hamming distance between hybrid and nonhybrid states is exaggerated because the hybrid cell can restrict the flow of information. This can lead to behavior like Figure 2, where rule 30 is hybridized with a single instance of rule 156. In this paper, two-dimensional cellular automata are studied to avoid this property.

Unfortunately, many previous studies of chaos control and hybrid cellular automata employ one-dimensional systems where this problem is apparent. In [3], a control of chaos system is implemented on a one-dimensional coupled map lattice system that acts over its two nearest neighbors, similar to a one-dimensional cellular automaton. Because it only acts over its two nearest neighbors, information can be restricted by a single hybrid cell or control pinning.

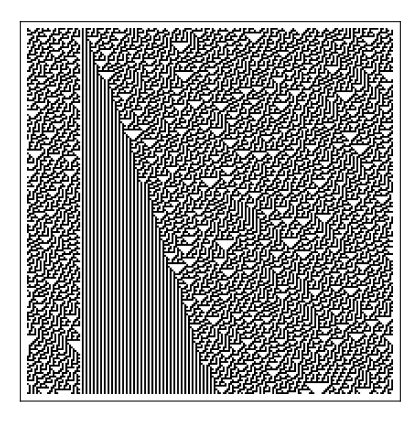


Figure 2. Elementary cellular automaton rule 30 hybridized with rule 156.

2. Methods

In this section, the method of hybrid cellular automata for manipulating complex and chaotic cellular automata is presented. Additionally, complexity measures are proposed as bounds to estimate the reachability of a system from various hybrid schemes.

2.1 Hybrid Cellular Automata for Manipulating Complex and Chaotic Systems

Cellular automata are governed by the exchange of information between locally interacting cells. Resulting from this, a cellular automaton attractor will be characterized from how information moves between the cells.

In chaotic and complex systems, perturbations may have nonlinear or critical effects. However, the effects of one small perturbation may cancel out another perturbation, and this is undesirable for developing robust control and manipulation techniques. In this situation, perturbations travel over the system's attractor.

A much more robust method is when the attractor actually changes. Hybrid cellular automata do this simply by changing the rules in certain locations, which causes the behavior of local points to differ. This will lead to different behavior in the unperturbed state, and thus the attractor has been modified.

As an example, an "attractor sample" of a 7×7 two-dimensional cellular automaton is compared with a 7×7 two-dimensional hybrid cellular automaton in Figure 3. The original system is the Game of Life cellular automaton; the modified system changes a single cell's rule with two-dimensional totalistic code 797.

An attractor sample is generated using a large set of random initial conditions, evaluated by the system for several iterations. The conditions are then enumerated, and the connections between input and output are put into a graph. For both systems, the same initial conditions are used to generate the graphs of their respective attractor samples.

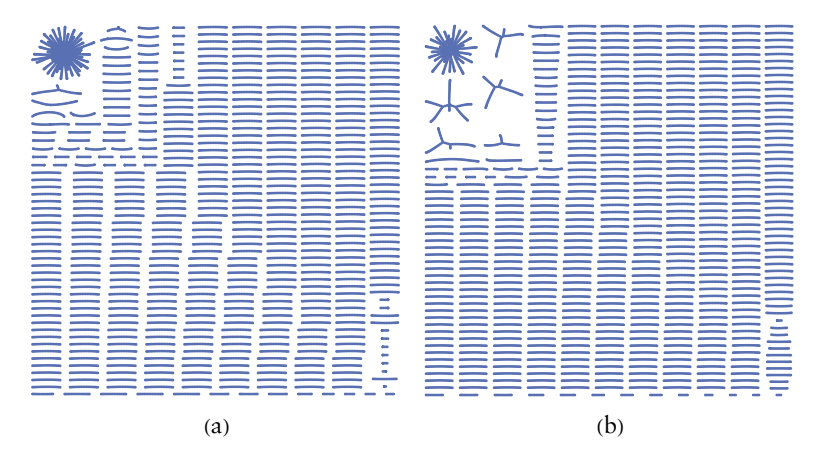


Figure 3. (a) An attractor sample of a 7×7 cellular automaton; and (b) a 7×7 hybrid cellular automaton using the same set of initial conditions.

2.2 Reachability of States and Complexity Measures

Many complex and chaotic systems will eventually thermalize into equilibrium states or limit cycles. For cellular automata, this means that the rate of formation and dissipation of structures within the system has become equal.

The equilibrium states and long-term behavior of these systems can be analyzed using different complexity measures. The measures are applied to the global state at each time step to analyze the dynamics of these systems with respect to time.

Four complexity measures are employed: block entropy, structural entropy, lossless compression and the block decomposition measure [4].

2.2.1 Block Entropy

Block entropy is the application of Shannon entropy [5] to a system decomposed into blocks of a predetermined size. Block entropy was first applied to study cellular automata in [6], where it was employed as a first predictor before other complexity measures were employed. The histograms of the block entropy of 6000 random binary strings of 200 bits are shown in Figure 4. This is done for block sizes of 5 and 10.

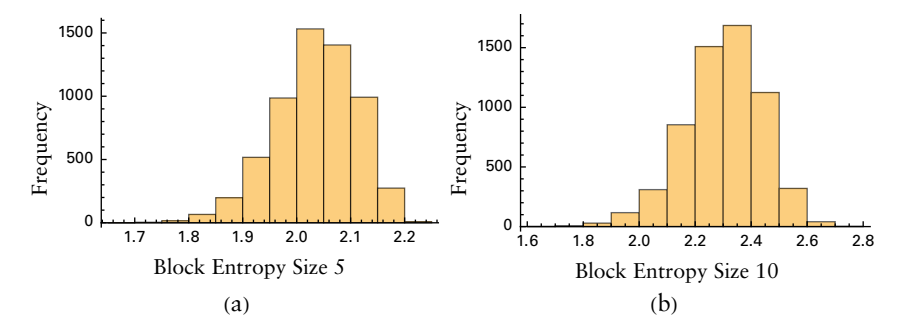


Figure 4. Histograms showing the distribution of 6000 random strings sorted by block entropy for: (a) size 5; and (b) size 10.

The Wolfram classes describe cellular automaton behavior as stable (class I), periodic (class II), chaotic (class III) or complex (class IV). Figure 5 shows the Wolfram classes with spacetime diagrams of different cellular automata. The horizontal axis shows space, while the vertical axis going down displays time. In Figure 5, (a) is stable, (b) is periodic, (c) is chaotic, and (d) is complex.

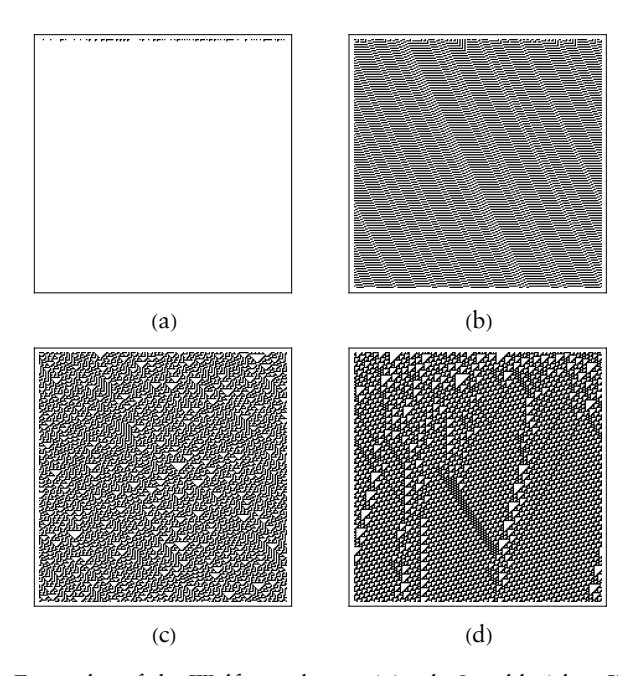
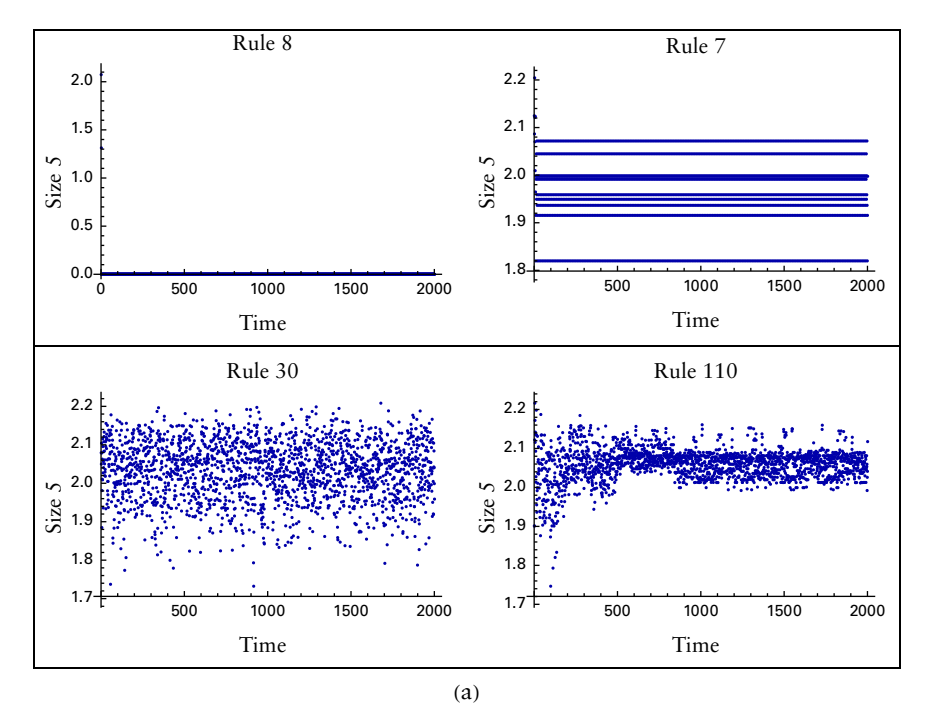
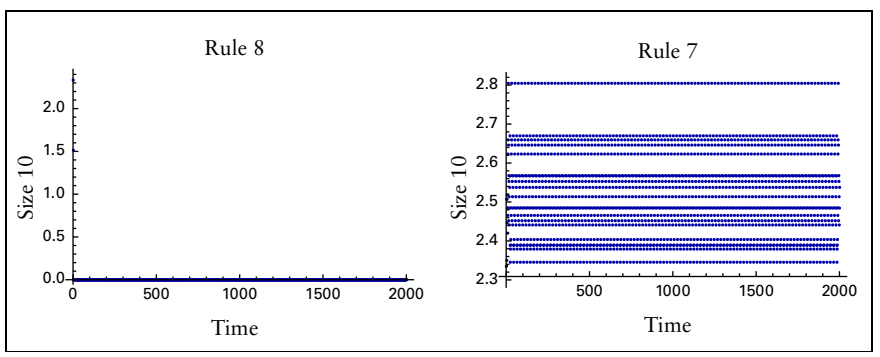


Figure 5. Examples of the Wolfram classes: (a) rule 8 stable (class I); (b) rule 7 periodic (class II); (c) rule 30 chaotic (class III); and (d) rule 110 complex (class IV).

For systems that form permanent structures, such as Wolfram class II and class IV systems, the shape of block entropy with respect to time will appear different for different sizes of block entropy. In Figure 6, the block entropy versus time for the four systems from Figure 5 is evaluated with a random string of 200 bits for 2000 time steps.

While the block entropy can be used to distinguish between the behavioral classes, the behavior trending toward equilibrium differs for both measurements for rule 110. When block entropy of size 5 is used, the behavior increases to an equilibrium level, while block entropy of size 10 shows a decrease to an equilibrium level.





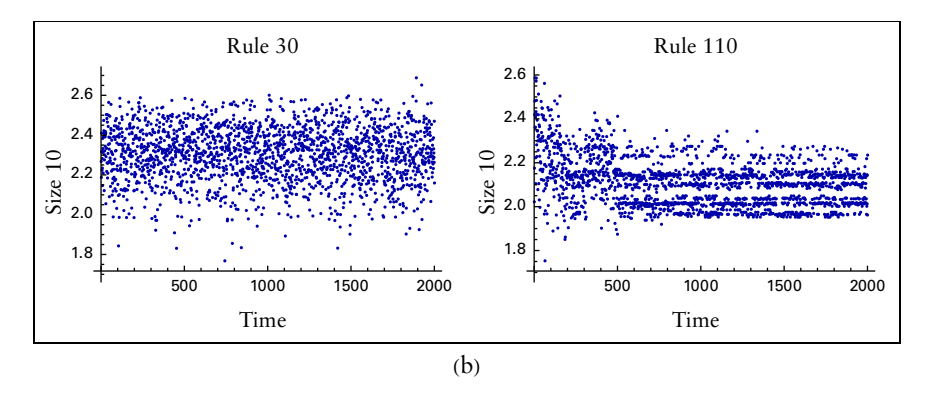


Figure 6. The block entropy of the example systems in Figure 5 run over 2000 iterations for: (a) block entropy size 5; and (b) block entropy size 10.

2.2.2 Structural Entropy

Structural entropy is a generalization of block entropy to blocks of nonuniform size. Unlike block entropy, structural entropy is not dependent upon measurement parameters.

Definition 1. Let a structure be defined as a group of cells adjacent to each other sharing the same value.

Structural entropy S is a measure of the total entropy of the structures present within a string. This is taken from the log of the multiplicity of the total number of unique combinations for which a string can be configured while preserving the size and count of structures within said string. Structures will only be preserved if they are next to their opposite color, so the multiplicity of configurations of each color can be separated. The multiplicities of both color structures M_W (white structure multiplicity) and M_B (black structure multiplicity) can be separated, as seen in

$$S = \log(M_W * M_B). \tag{1}$$

The multiplicity of each color is found by finding the total multiplicity of all possible structures, then removing the duplicates. This is done by taking the factorial of the total number of structures and dividing by the product of the factorials of the count of occurrences of each structure. The structural multiplicity M of a color is expressed in equation (2).

Definition 2. Let A be the total number of structures and D be the list containing the occurrences of each structure:

$$M = \frac{A!}{\prod_{n=1}^{A} D_n!}.$$
 (2)

In Figure 7, a histogram shows the structural entropy of 6000 random strings of 200 bits. It can be observed that the average is around 115, with a deviation of around 5. The left skew is due to the fact that there is a maximal structural entropy for strings of finite size.

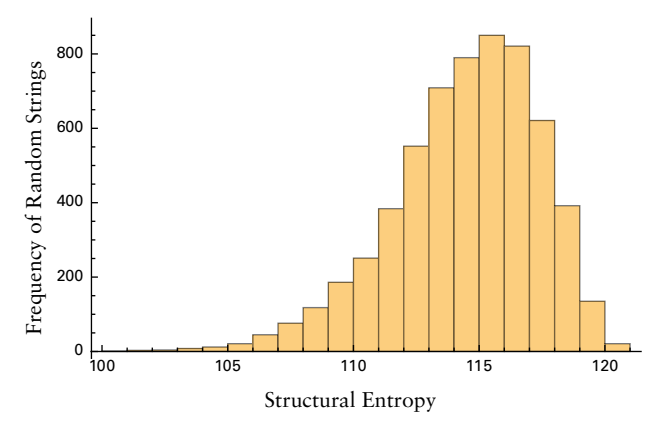
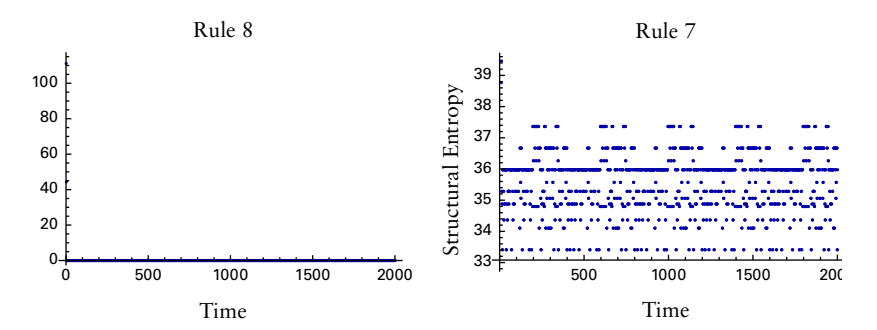


Figure 7. A histogram of the structural entropy of strings of size 200 bits.

The plots in Figure 8 show the example structural entropy applied to the example systems from the four Wolfram classes [7]. For each cellular automaton shown in Figure 6, random strings of 200 bits are generated and then run for 2000 iterations. (The class I system is only shown for 20 iterations to emphasize its transition to stability.) For each iteration, the structural entropy is measured.

Similarly to block entropy, the behavior of structural entropy with respect to time varies considerably for each of the systems shown above. Class I and II systems are trivially distinguishable by the drop to a constant structural entropy and oscillations, respectively.

Class III systems appear random with respect to time, showing an average similar to the average structural entropy for random strings. The distribution matches up quite well with the distribution for randomly generated strings.



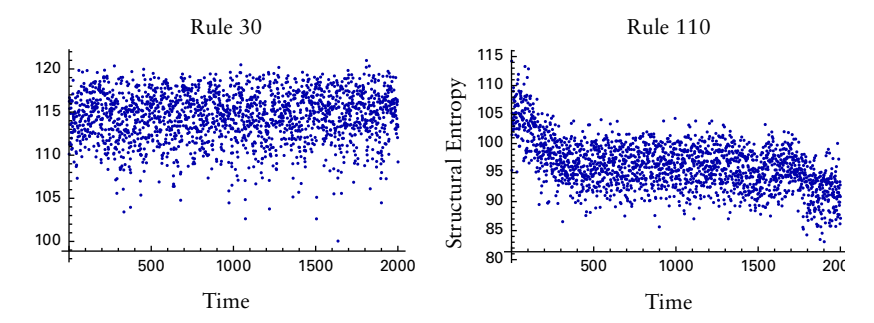


Figure 8. Structural entropy of the systems shown in Figure 6 run over 2000 iterations of time.

From random initial conditions, class IV systems will drop to an equilibrium level of structure formation until they appear to be bounded above. It can be observed that the structural entropy of rule 110 in the plot drops to a maximum of around 100. This can be useful for estimating whether or not states will be reachable from a given configuration.

Multidimensional structural entropy is implemented by flattening the two-dimensional state and taking the one-dimensional structural entropy of the string.

2.2.3 Compression Measures

Compression has also been employed to study the complexity of cellular automata. Compression was the first qualitative non-entropy-based measure used to study the behavior of cellular automata [4].

Figure 9 shows a histogram of the compressed size of 6000 random strings of 200 bits. It can be observed that the average is around 170, with a deviation of around 7. It is notable how the bin sizes are much larger for the compression metric.

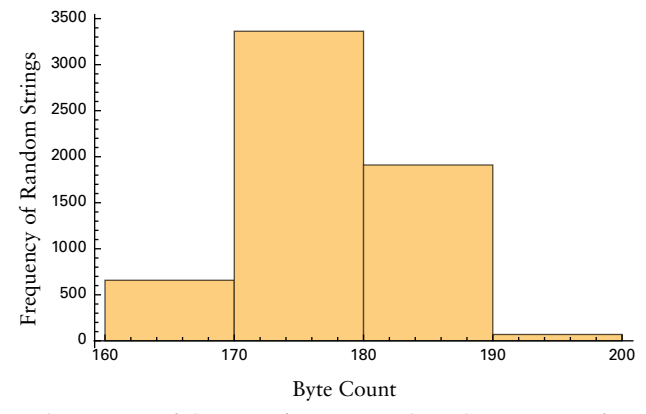


Figure 9. A histogram of the size of compressed random strings of 200 bits.

2.2.4 Block Decomposition Method

The block decomposition method (BDM) [4] is a method for estimating algorithmic complexity of large objects. It decomposes a large object into a set of blocks with known algorithmic complexity, then applies a grading based upon the algorithmic complexity of the block along with its frequency.

Figure 10 shows a histogram of the BDM measure of 6000 random 20×20 blocks. It can be observed that the BDM measure is notably less skewed than the other measures analyzed thus far.

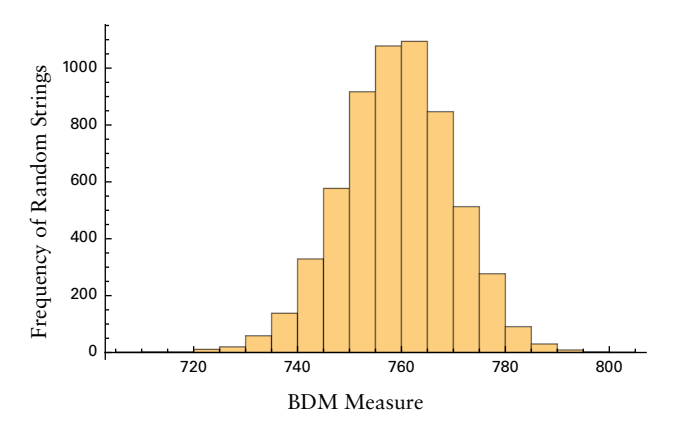


Figure 10. A histogram of the BDM measures of 6000 random 20×20 blocks.

2.2.5 Comparison of Methods

While all four methods have the ability to distinguish between the behavior classes of cellular automata, some measures can detect more details than others. To compare measures, a Wolfram class III structural oscillator is examined.

A structural oscillator is a system that oscillates between randomness and structure formation; however, the structures are unrelated to each other. No information is effectively transmitted in class III systems. Figure 11 shows the structural oscillator for the first four time steps.

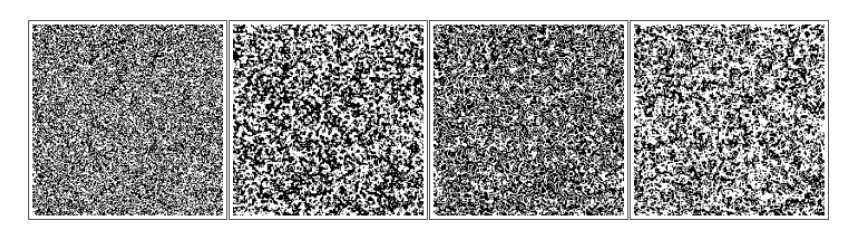


Figure 11. The first four steps of the two-dimensional totalistic cellular automaton rule 797: a structural oscillator.

The four complexity measures are compared in Figure 12 for the first 50 time steps of the structural oscillator.

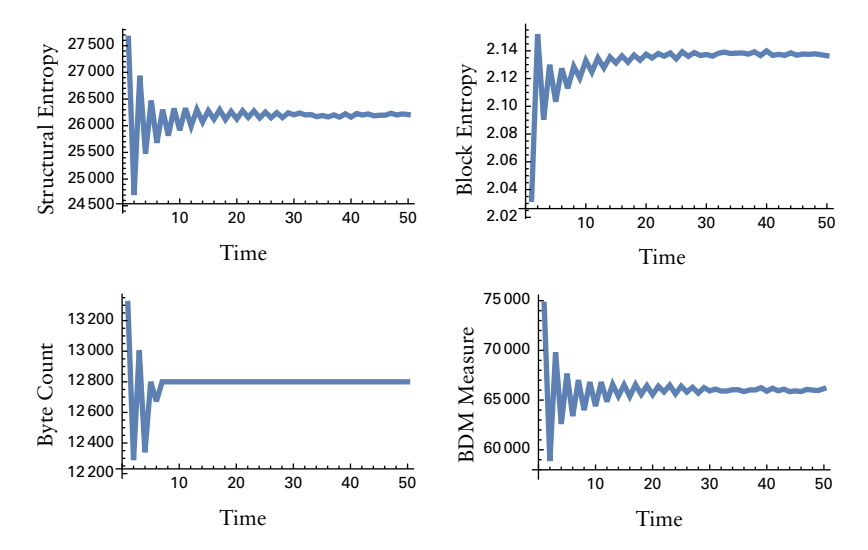


Figure 12. The four complexity measures applied to the structural oscillator shown in Figure 11.

Structural entropy and the BDM identify this structural oscillation and display similar trends of damped oscillation toward a mean. Compression also captures this somewhat; however, after enough time steps, no distinction is found. Block entropy captures some oscillation; however, it shows the equilibrium state as having greater complexity than the initial conditions.

3. Results

This section shows the results of two experiments measuring the impact of measurement uncertainty on hybrid cellular automata. Additionally, an example application of hybrid cellular automata is shown, and the ability of the complexity measures to predict the reachability of hybrid systems is examined. Finally, the ability of hybrid schemes to affect system dynamics is examined.

3.1 Performance of Hybrid Cellular Automata with Measurement Uncertainty

To analyze the impacts of hybrid cellular automata, a perturbation analysis [8] is performed. Perturbation analyses use perturbations to study the algorithmic information dynamics [9] in complex systems

and can be employed to attempt to reconstruct a phase space from incomplete information. Here, the effect of perturbations introduced into the initial conditions of hybrid cellular automata is compared with perturbations introduced into a control system.

Initially a control initial condition (75×75) is prepared and run over 20 iterations. This initial condition is then perturbed by a single cell 200 different times. The set of perturbed initial conditions is then evaluated over 20 iterations, then the absolute differences between the final perturbed states and the final control state are taken, then this is averaged for all perturbed states. This is performed for both the hybrid system and the control system. The control system is simply the Game of Life cellular automaton, while the hybrid rule is code 797.

Figure 13 shows the averaged absolute differences between the control system and hybrid system after 20 iterations. Darker-colored cells indicate a higher probability of that cell changing. For reference, a scale at the top of the figure shows the probability of cells changing ranging from 0 (white far left) to 100% (black far right). The red dot in Figure 13(b) shows the location of the hybrid cell.

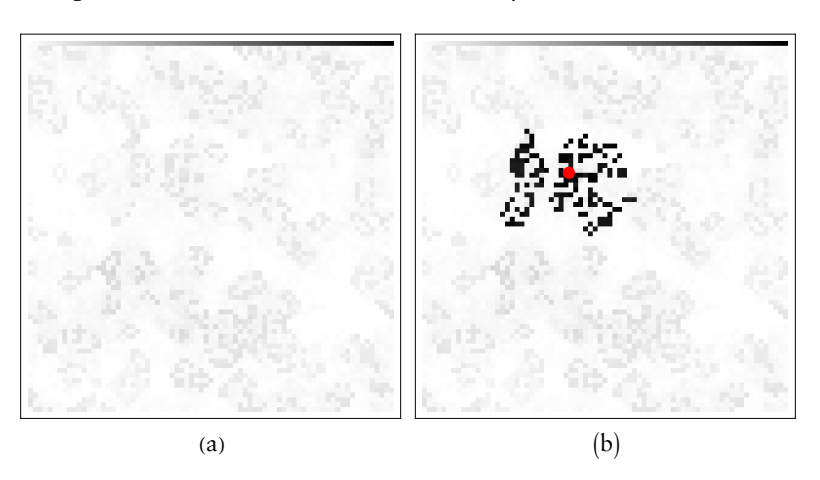


Figure 13. The averaged difference between perturbed states and control states for: (a) the uniform cellular automata; and (b) the hybrid cellular automata.

It can be observed that the hybrid cell (as shown in Figure 13(b)) has a region surrounding itself where the probability of the cells changing is significantly high. This can be attributed to the modified attractor.

3.2 Hybrid Systems in Varying Levels of Uncertainty

In this section, the certainty of changes caused by hybrid systems is examined as the total number of perturbations of initial conditions of the system is varied.

Initially a control initial condition (75×75) is prepared and run over 20 iterations. In Figure 14, three sets of perturbations are shown; the first set has been perturbed in a single instance, the second set in five instances, and the third in 10 instances.

Each set of perturbed initial conditions is then evaluated over 20 iterations, then the absolute differences between the final perturbed states and the final control state are taken, then this is averaged over all perturbed states for each set. This is performed for both the control system and the hybrid system.

Similarly to Figure 13, a scale at the top of the each plot shows the probability of cells changing ranging from 0 (white far left) to 100% (black far right). Additionally, a red dot marks the location of the hybrid cell.

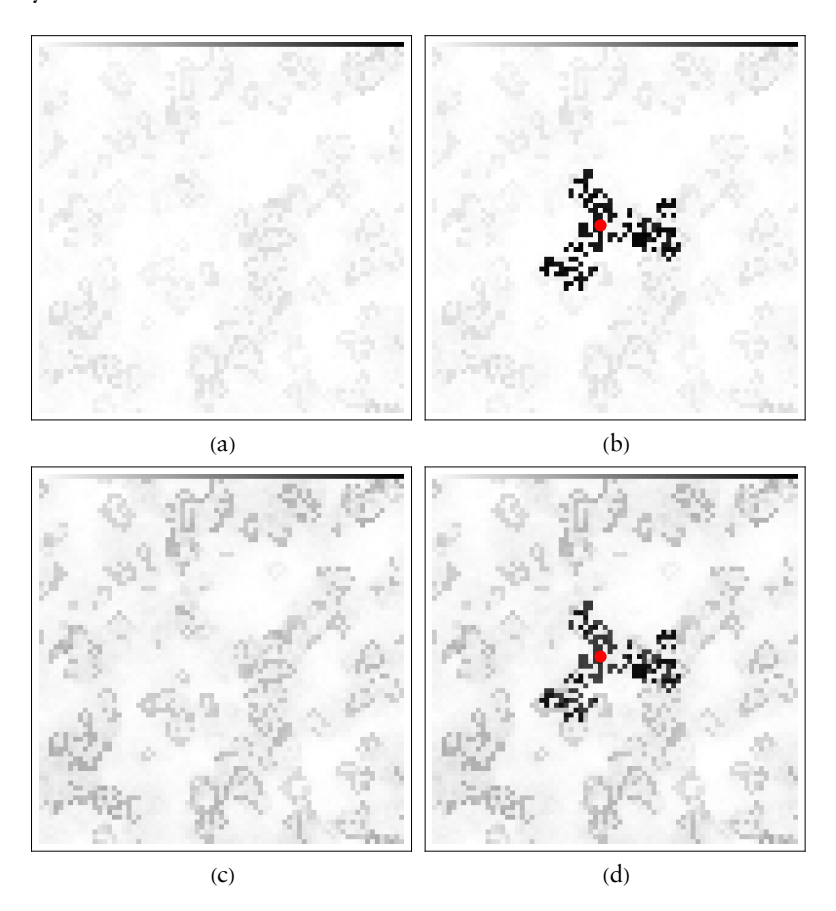


Figure 14. (continues).

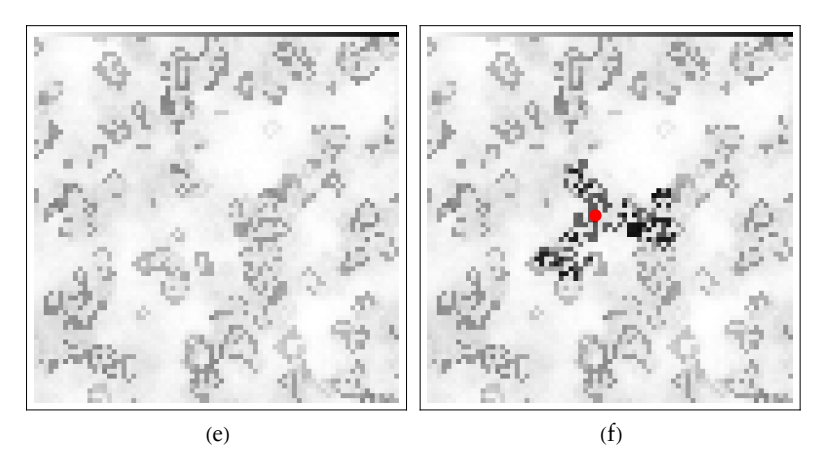


Figure 14. The averaged differences between perturbed states and control states for the control system (left) and hybrid system (right) with 1 perturbation (top), 5 perturbations (middle), 10 perturbations (bottom).

It is important to observe that as the total number of perturbations increases, the probability of some cells changing and the respective structures forming increases. This is partially due to the higher surface area the perturbations occupy, leading to a higher probability of changing the same states. Also, this is partially due to some different states evolving into the same final result.

As found with the control system, the probability of some states changing and respective structures forming increases as the total number of perturbations is increased. It can be observed that the hybrid changes are still present and generally are more probable than changes due to random environmental perturbations.

It is important to note that perturbations that occur near hybrid cells will have an impact on the hybrid behavior, leading to uncertainty regarding which cells change. This will decrease the effectiveness of the hybrid perturbations, so it is important to have accurate measurements and minimize potential error near regions of active hybridization.

3.3 Applied Example: Manipulating the Belousov–Zhabotinsky Reaction

In this section, the method of hybrid cellular automata for manipulating chaotic systems is applied to the Belousov–Zhabotinsky reaction [10]. The Belousov–Zhabotinsky reaction is an oscillating chemical reaction that displays nonlinear chaotic behavior. When placed upon a microemulsion, it can be characterized by growing swirls that replace each other; a good demonstration of this is available in [11]. In this demonstration, the Belousov–Zhabotinsky reaction on a microemulsion is modeled using cellular automata.

Control of chaos methods have been implemented for this reaction [12]; however, these control methods deal with controlling global properties, while the applications of hybrid cellular automata focus on implementing specific local changes. A direct parallel can be drawn between the application of hybrid cellular automata and placing physical reagents.

To start, a control experiment is done under random initial conditions (200×200) and evolved for 90 steps (Figure 15). For real-world applications, this will serve as our idealized model based upon the knowledge of our setup.

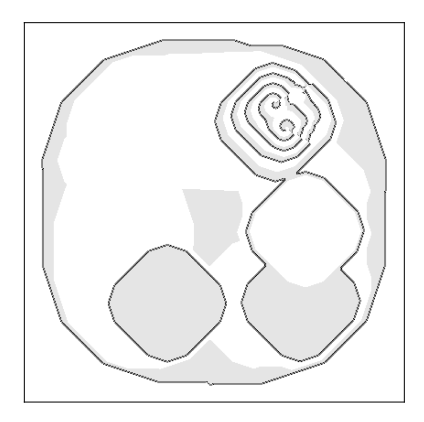


Figure 15: The final state of the control evaluation for the Belousov–Zhabotinsky reaction.

Random perturbations are then added to the initial conditions to analyze common ways the system will deviate from the initial setup when perturbed. It can be observed in Figure 16 that there are many possibilities for squarish regions (similar to the ones shown in Figure 15) forming along the unoccupied upper-left region. A scale at the top of the each plot shows the probability of cells changing ranging from 0 (white far left) to 100% (black far right).

Next, hybrid cells are scattered throughout the rule matrix to start to understand patterns that are reachable from hybrid perturbation. This is evaluated over the same set of perturbations used in the perturbed control trial done in Figure 16. The results of the hybridization are shown in Figure 17.



Figure 16. The averaged difference between the control state and perturbed states.



Figure 17. The averaged difference between the control state and perturbed states run through a hybrid scheme.

From the random sparse hybridization, it can be seen that patterns are likely to form in radial blobs or along edges. The radial blobs can be chosen as a basis for implementing change in the Belousov–Zhabotinsky reaction.

Control plans can be drawn up by finding the most effective methods for implementing radial blobs. A square block of hybrid cells is analyzed with respect to the perturbations previously employed (Figure 18). The pattern is found satisfactory, so it will be employed as a basis for constructing more interesting changes.

Because cellular automata have local interactions, superposition (prior to the mutual interaction of modified hybrid behavior) can be employed when constructing patterns. If the desired pattern is concentric circles, this can be approximated by arranging the hybrid blocks in a circular formation.

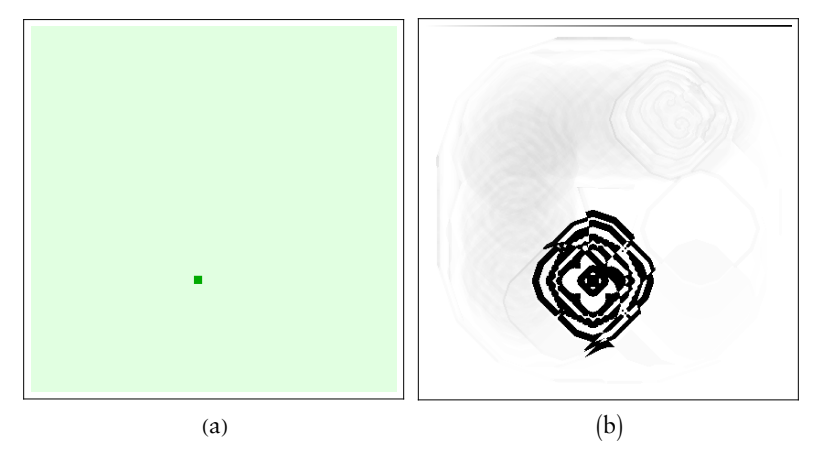


Figure 18. The rule configurations of: (a) a hybrid basis; and (b) its average difference between the control state and perturbed states run through the hybrid scheme.

The behavior of the system after the mutual interaction of hybrid patterns varies significantly according to synchronization as well as environmental factors (Figure 19). Synchronization is easy to control by adjusting the distance between the hybrid structures; however, environmental factors are often uncontrollable and can be difficult to resolve.

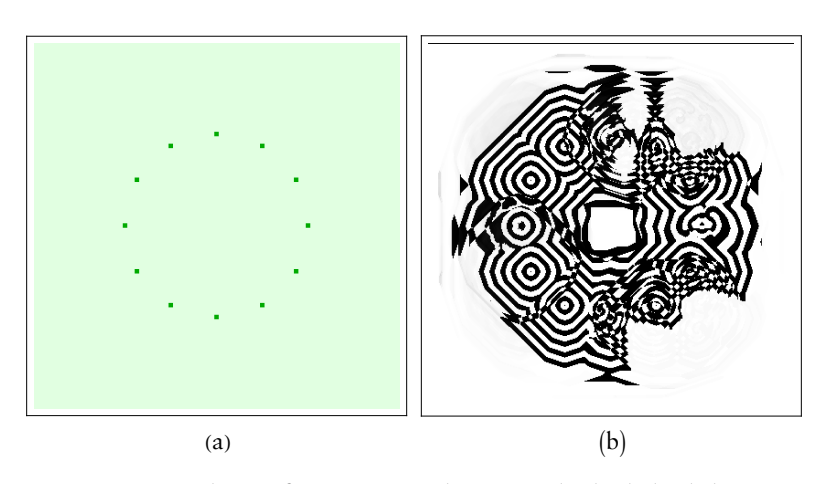


Figure 19. A rule configuration employing multiple hybrid basis states: (a) arranged in a circle; and (b) its average difference between the control state and perturbed states run through this hybrid scheme.

To resolve this, a different basis can be employed that interacts differently with its environment. Before attempting to manipulate a system, it is wise to have a large and varied hybrid basis.

Figure 20 shows the final output state of the control initial condition run through the hybrid scheme in Figure 19. Concentric circles are approximated around the inner ring and outer ring.

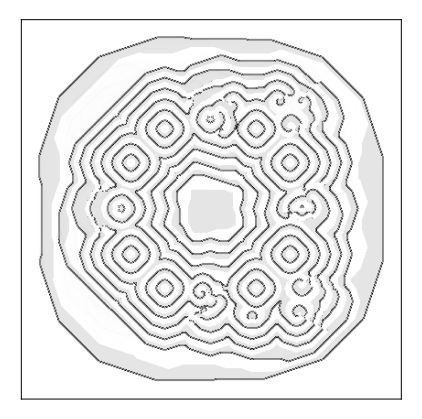


Figure 20. The final state of the control initial condition, run through the hybrid scheme from Figure 17.

3.4 Complexity Measures for Qualifying Reachable States

This experiment studies the effect of hybridization on the complexity measures. Specifically, the purpose of this experiment is to understand which complexity measures can provide an estimate of the reachability of states under realistic hybrid schemes and also see how hybrid schemes impact dynamics.

Obviously, this will depend on the concentration of hybrid cells. In the context of the systems that hybrid cellular automata should be applied to, the total concentration of cells from the original system should dominate over the concentration of hybrid cells.

In Figure 21, five different hybrid schemes are compared for their ability to affect the complexity measures. The first hybrid scheme features an instance of a single hybrid cell. The second hybrid scheme features a sparse spread of cells over the entire map. The third hybrid scheme features a clustering of hybrid cells concentrated near the center. The fourth hybrid scheme expands the size of the hybrid perturbations, establishing large clusters of hybrid cells. The fifth hybrid scheme features a much denser spread of hybrid cells. The control system is the Game of Life cellular automaton, while the hybrid system is code 797.

First a set of 200 random initial conditions is generated; each hybrid scheme is then evaluated over each initial condition for 75 steps. The average and standard deviations of the four measures applied for each scheme are plotted in Figures 22 and 23.

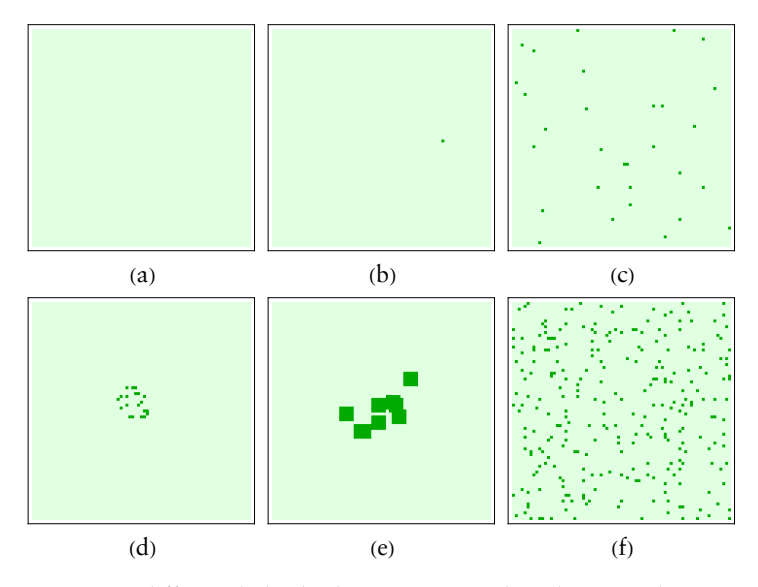


Figure 21. Five different hybrid schemes compared to the control: (a) control; (b) single hybrid cell; (c) sparse spread of hybrid cells; (d) localized concentration; (e) large clusters; and (f) a high concentration of randomly distributed hybrid cells.

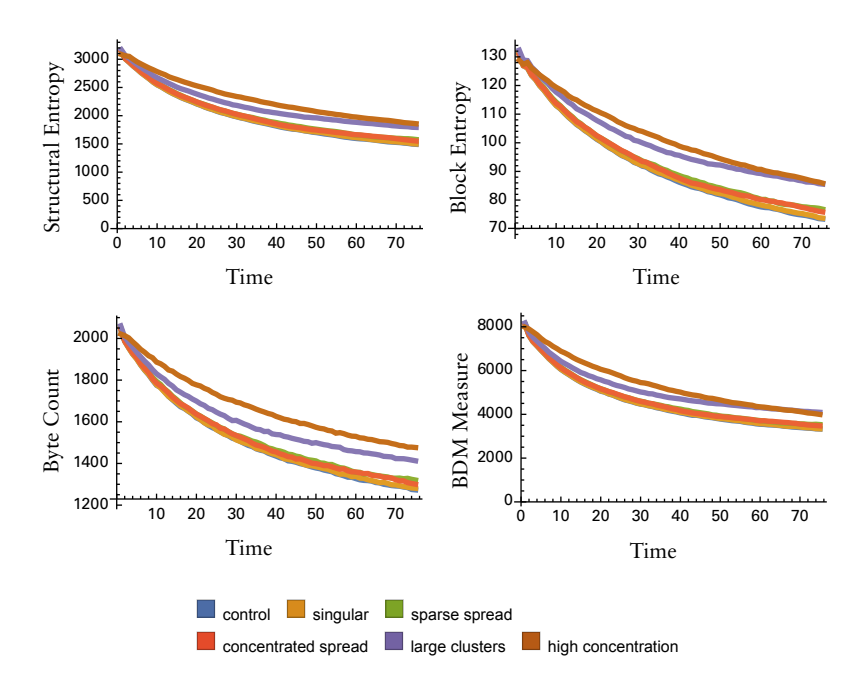


Figure 22. The average of the complexity measures for the 200 random initial conditions run through each hybridization scheme.

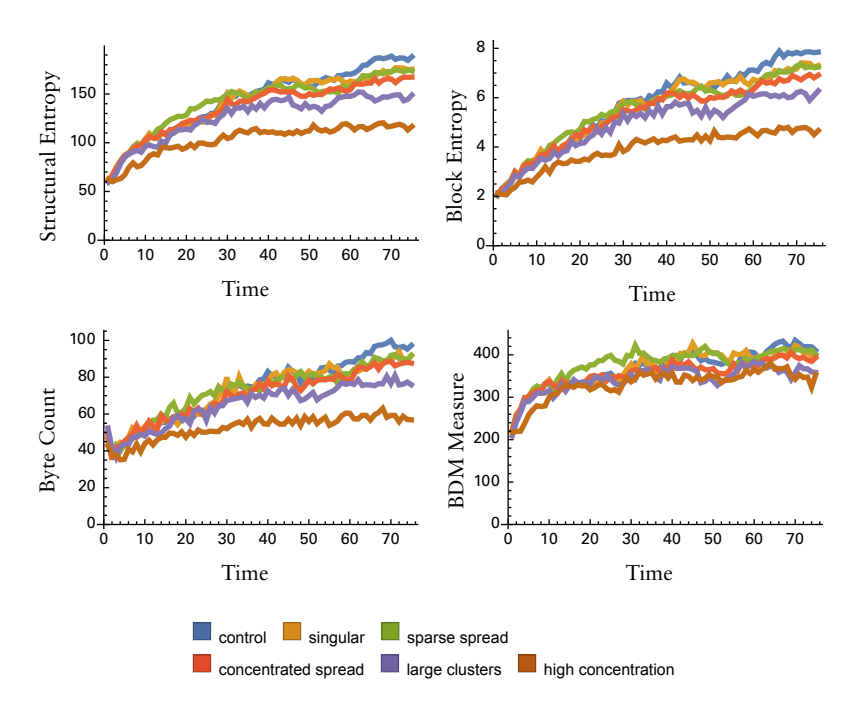
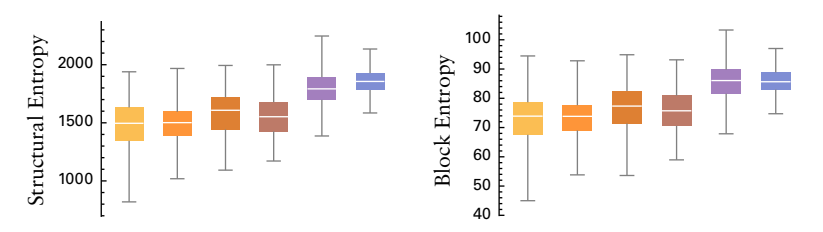


Figure 23. The standard deviation of the complexity measures for the 200 random initial conditions run through each hybridization scheme.

It can be noted that the measures all act similarly to each other. Out of all hybrid schemes, generally the control hybrid scheme has the highest standard deviation, while the high-concentration system has the lowest. This trend continues for the other schemes: the standard deviations appear in roughly the same places as they do in the other measures. The notable exception is the BDM measure, where the standard deviations are grouped together.

The terminating value of a system tells us the measured value of the final evaluated state after a set number of evaluations. The ranges of terminating values for each complexity measure are plotted for each hybrid scheme in Figure 24.



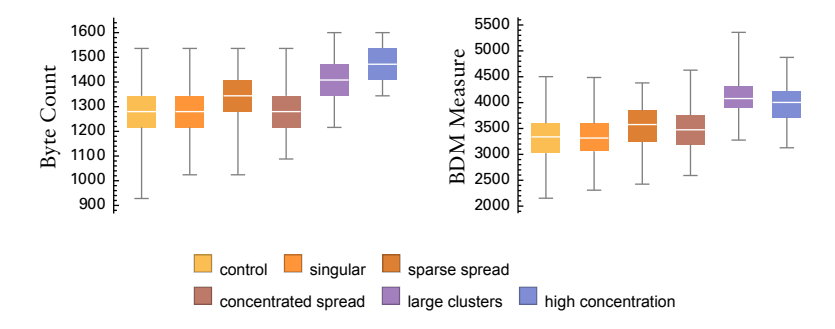


Figure 24. Box plots showing the distribution of terminating values of the four complexity measures for the six cases of hybridization.

The range for the control system spans over almost all of the other ranges, with the notable exception of the large cluster hybrid scheme and the high-concentration scheme. This is most likely due to the high quantity of hybrid cells, which would actually shift the average of these measures. Sometimes the sparse spread system exceeds the boundaries of complexity, however, not by much.

Compression shows that the large clusters and high-concentration systems exceed the bounds of the control system; however, this effect is not very pronounced. BDM displays the highest deviation where large clusters far exceed the control range; however, the high-concentration scheme is less pronounced. Structural entropy and block entropy are similar in this assessment.

3.5 Analysis of the Dynamics of Deviating Hybrid Schemes

In [4], phase transitions of cellular automata are studied using compression and gray codes to analyze the dynamics with respect to different initial conditions. In this section, the time dynamics of BDM and structural entropy for the high-impact hybrid schemes are analyzed with respect to the complexity of the initial conditions.

The selected hybrid schemes exceeded the bounds of complexity outlined by the control system in the previous experiment. The candidates are the sparse spread scheme, the cluster scheme and the high-concentration scheme. These are shown in Figure 25 with respect to a control system. The light green represents the control rule (Game of Life), while the dark green shows the hybrid rule (code 797).

Initial conditions are generated according to their complexity, using a hybrid cellular automaton applied to random initial conditions. Elementary cellular automaton rule 8 is hybridized with rule 7, and the probability of cells that are rule 7 is varied up to a maximum of 0.5. The hybrid system is then evaluated for 20 steps, and the final

state is taken as the initial condition. The conditions are then partitioned into a 75×75 grid of binary initial conditions.

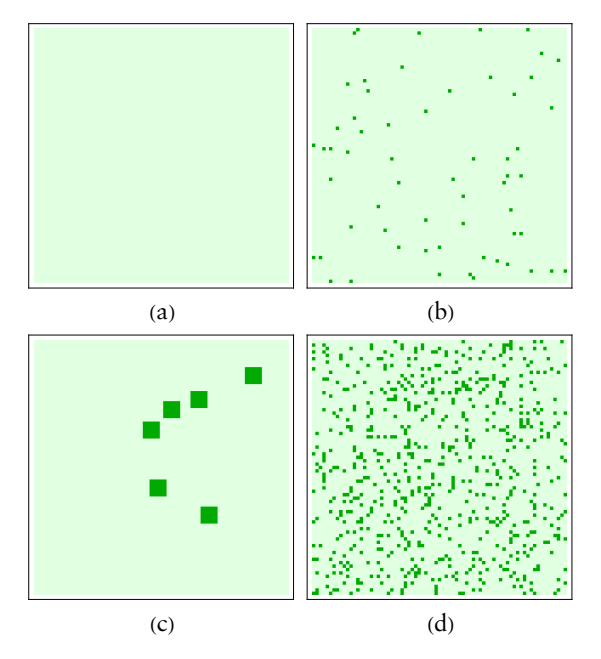


Figure 25. The control state and three hybrid schemes found to exceed the bounds of the control state: (a) control state; (b) sparse spread; (c) clusters; and (d) high concentration.

Initial conditions are generated according to their complexity, using a hybrid cellular automaton applied to random initial conditions. Elementary cellular automaton rule 8 is hybridized with rule 7, and the probability of cells that are rule 7 is varied up to a maximum of 0.5. The hybrid system is then evaluated for 20 steps, and the final state is taken as the initial condition. The conditions are then partitioned into a 75×75 grid of binary initial conditions.

The BDM measure and the structural entropy with respect to the proportion of hybrid cells are shown in Figure 26. It can be noted that the BDM measure has a different initial concavity than the structural entropy. This is because the simpler conditions have a lower Kolmogorov complexity, which decreases the rate of change of the BDM measure.

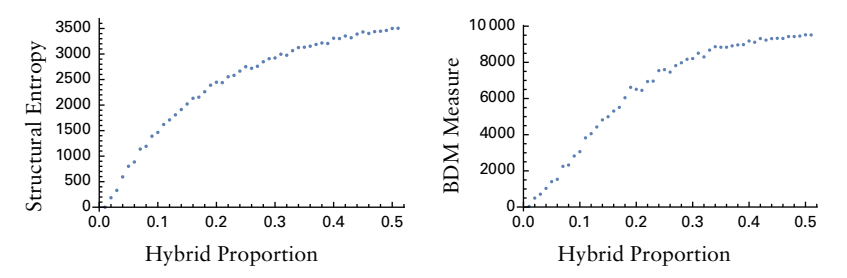


Figure 26. The structural entropy and BDM measure compared with respect to the hybrid proportion for generated initial conditions.

Initially, five hybrid distributions are chosen along the curve in Figure 26. For each distribution, 200 random initial conditions are generated. These initial conditions are then run over the hybrid schemes (Figure 27), after which BDM and structural entropy measures are applied (Figure 28). The measures are averaged for each distribution group, and the behavior of the complexity measures is analyzed with respect to time.

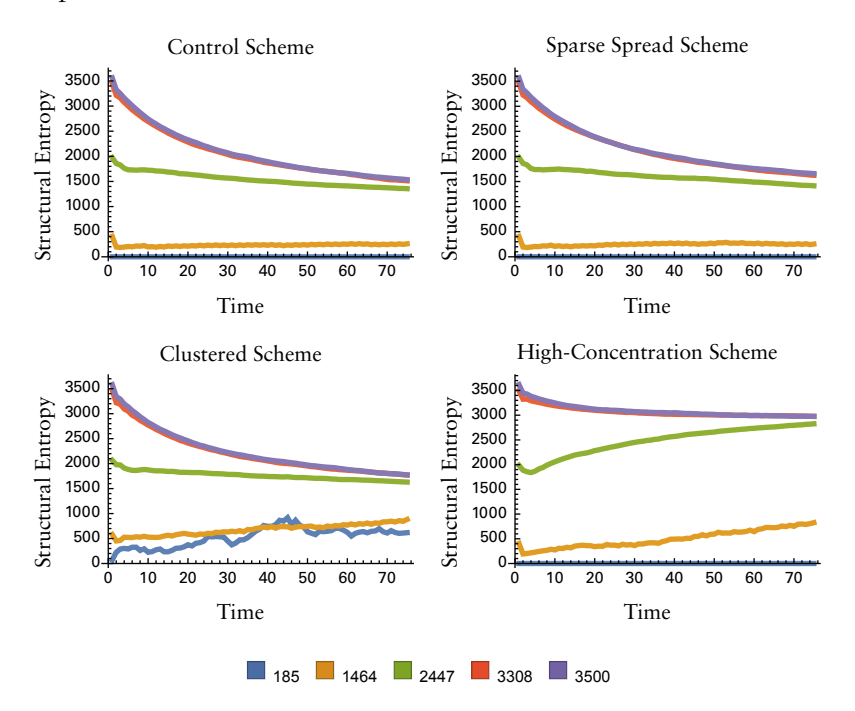


Figure 27. The four schemes compared with initial conditions of different structural entropies. The colors of the lines correspond to the structural entropy of the initial condition shown in the legend on the bottom.

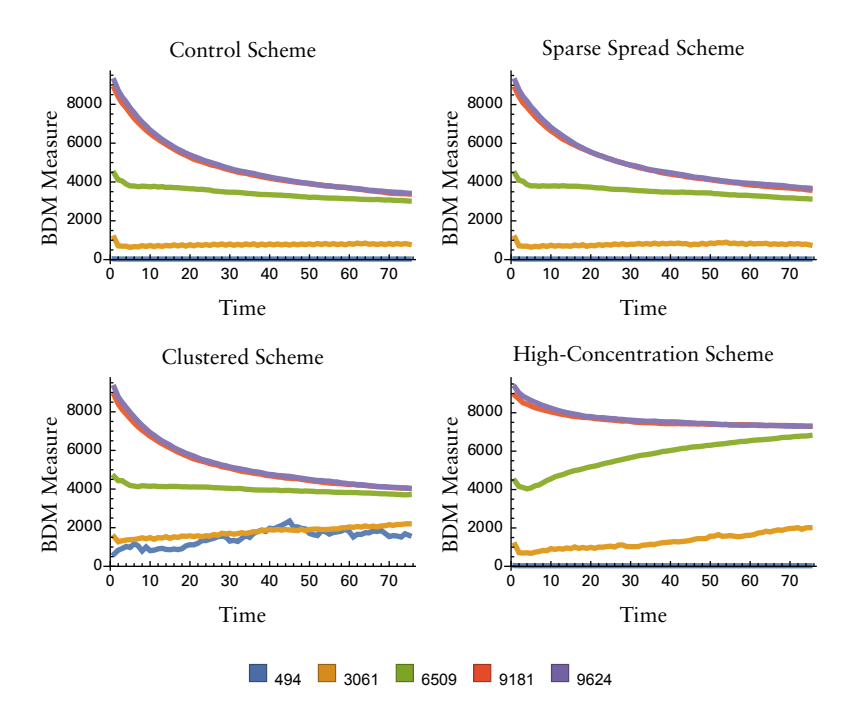


Figure 28. The four schemes compared with initial conditions of different BDM measures. The colors of the lines correspond to the BDM measure of the initial condition shown in the legend on the bottom.

The sparsely distributed system shows little deviation from the control system with its dynamic behavior. This was partially expected, as it did not deviate as much as the other hybrid schemes.

The high-concentration scheme seems to raise the average complexity levels; however, it seems to affect most states the same way. The cluster scheme is much more interesting, because the behavior of high-complexity states seems unchanged with respect to the control; however, the lower-complexity states are changed. The minimal-complexity states are elevated compared to the other hybrid schemes. This is most likely because the hybrid systems have enough space in the clusters to produce their own structures, which dissipate into the environment.

It can be noted that structural entropy and the BDM measure behave extremely similarly in this application.

4. Discussion

Hybrid cellular automata have demonstrated their ability to create certain changes that can withstand initial measurement error or environmental perturbations. As the environmental error increases, the probability of certain other states occurring also increases. This can compete with hybrid changes at large enough error concentrations. However, as hybrid systems modify an attractor, generally the hybrid changes will be hardy to measurement error in the initial conditions.

When manipulating chaotic systems using hybrid cellular automata, the principle of superposition can be applied to hybrid differences. Thus, hybrid control can be developed using basis functions of hybrid states. An appropriate hybrid basis can be applied for time steps similar to the Lyapunov time, effectively reducing the total amount of computation required to construct control algorithms.

The complexity measures seems to bound reasonable hybrid changes to a system. In the third experiment, it was observed that only the hybrid schemes with high concentrations of hybrid cells were able to exceed the bounds of these measures from the control state. Then it was found in the fourth experiment that these systems were able to modify the general dynamic behavior of the system with respect to the complexity of the initial conditions.

This would suggest that these complexity measures can be employed to find hybrid schemes that significantly change the dynamics with respect to the control. It was found that the clusters had the highest deviation from the range of the control system across all measures, and the clusters displayed the most interesting behavior.

4.1 Future Work

It is known that many cellular automata can emulate each other from a fixed perturbation [13]. This effectively allows cellular automata to compile other cellular automata. The use of hybrid cellular automata to compile other systems can be studied to implement chaos control algorithms in larger dynamic systems.

Additionally, the connection between structural entropy and the block decomposition method (BDM) measure should be further explored.

References

- [1] T. Miyoshi and Q. Sun, "Control Simulation Experiment with Lorenz's Butterfly Attractor," *Nonlinear Processes in Geophysics*, **29**(1), 2022 pp. 133–139. doi:10.5194/npg-29-133-2022.
- [2] M. Rajasekar and R. Anbu, "Characterization of Uniform and Hybrid Cellular Automata with Reflecting Boundary," *Journal of Physics: Conference Series*, **1850**, 2020 012128. doi:10.1088/1742-6596/1850/1/012128.

[3] H. Gang and Q. Zhilin, "Controlling Spatiotemporal Chaos in Coupled Map Lattice Systems," *Physical Review Letters*, 72(1), 1994 pp. 68–71. doi:10.1103/PhysRevLett.72.68.

- [4] H. Zenil, "Compression-Based Investigation of the Dynamical Properties of Cellular Automata and Other Systems," *Complex Systems*, 19(1), 2010 pp. 1–28. doi:10.25088/ComplexSystems.19.1.1.
- [5] C. E. Shannon, "A Mathematical Theory of Communication," *The Bell System Technical Journal*, 27(3), 1948 pp. 379–423. doi:10.1002/j.1538-7305.1948.tb01338.x.
- [6] H. Zenil and E. Villarreal-Zapata, "Asymptotic Behavior and Ratios of Complexity in Cellular Automata," *International Journal of Bifurcation* and Chaos, 23(09), 2013 1350159. doi:10.1142/S0218127413501599.
- [7] S. Wolfram, A New Kind of Science, Champaign, IL: Wolfram Media, Inc., 2002.
- [8] H. Zenil, N. A. Kiani, F. Marabita, Y. Deng, S. Elias, A. Schmidt, G. Ball and J. Tegner, "An Algorithmic Information Calculus for Causal Discovery and Reprogramming Systems," iScience, 19, 2019 pp. 1160–1172. doi:10.1016/j.isci.2019.07.043.
- [9] H. Zenil, N. A. Kiani and J. Tegnér, Algorithmic Information Dynamics: A Computational Approach to Causality with Applications to Living Systems, New York: Cambridge University Press, 2023.
- [10] C. Gray, "An Analysis of the Belousov–Zhabotinskii Reaction," *Rose-Hulman Undergraduate Mathematics Journal*, 3(1), 2002 1. scholar.rose-hulman.edu/rhumj/vol3/iss1/1.
- [11] L. Zammataro. "Idealized Belousov-Zhabotinsky Reaction" from the Wolfram Demonstrations Project—A Wolfram Web Resource. demonstrations.wolfram.com/IdealizedBelousovZhabotinskyReaction.
- [12] V. Petrov, V. Gáspár, J. Masere and K. Showalter, "Controlling Chaos in the Belousov-Zhabotinsky Reaction," *Nature*, 361(6409), 1993 pp. 240–243. doi:10.1038/361240a0.
- [13] J. Riedel and H. Zenil, "Cross-Boundary Behavioural Reprogramma-bility Reveals Evidence of Pervasive Universality," *International Journal of Unconventional Computing*, **13**(4–5), 2018 pp. 309–357. www.oldcitypublishing.com/journals/ijuc-home/ijuc-issue-contents/ijuc-volume-13-number-4-5-2018/ijuc-13-4-5-p-309-357.